

Chromaticity effects in microlensing by wormholes

Ernesto Eiroa^{1,*}, Gustavo E. Romero^{2,†} and Diego F. Torres^{2,‡}

¹ Instituto de Astronomía y Física del Espacio, C.C. 67, Suc. 28, 1428, Buenos Aires, Argentina

² Instituto Argentino de Radioastronomía, C.C.5, 1894 Villa Elisa, Buenos Aires, Argentina

October 26, 2018

Abstract

Chromaticity effects introduced by the finite source size in microlensing events by presumed natural wormholes are studied. It is shown that these effects provide a specific signature that allow to discriminate between ordinary and negative mass lenses through the spectral analysis of the microlensing events. Both galactic and extragalactic situations are discussed.

arXiv:gr-qc/0104076v1 24 Apr 2001

*e-mail: eiroa@iafe.uba.ar

†Member of CONICET; e-mail: romero@irma.iar.unlp.edu.ar

‡e-mail: dtorres@venus.fisica.unlp.edu.ar

1 Introduction

A wormhole is a region of space-time with non-trivial topology. It has two mouths connected by a throat. The mouths are not hidden by event horizons, as in the case of black holes, and, in addition, there is no singularity that could avoid the passage of particles from one side to the other. After the pioneering paper by Morris & Thorne [1], wormhole solutions to the Einstein field equations has been extensively studied in the literature (see Refs. [2] and references cited therein).

Static wormhole structures require the violation of the average null energy condition in the wormhole throat in order to exist. Plainly stated, this means that the matter threading the wormhole must exert gravitational repulsion to stay stable against collapse. Although there are known violations to the energy conditions (e.g. the Casimir effect), it is currently far from clear whether large macroscopic amounts of “exotic matter” exist in the nature. If natural wormholes actually exist in the universe (e.g. if the original topology after the Big-Bang was multiply connected), then there should be observable electromagnetic signatures that could lead to their identification.

Cramer et al. [3] and Torres et al. [4] have recently studied the microlensing effects of a negative mass (e.g. a natural stellar-size wormhole) on the light from a background point-like source [for a macrolensing study see [5]]. These authors have shown that the typical lightcurves expected from microlensing events produced by wormholes should be very different from the lightcurves in ordinary (positive mass) microlensing of point sources. In the standard case, a time symmetric burst in the flux density from the background source occurs. If the lens, instead, is a wormhole, the gravitational repulsion creates an obscure umbra region, deflecting light rays that should, otherwise, reach the observer. The wormhole basically acts as a divergent lens. However, light is concentrated on the border of the umbra region producing two separated intensity enhancements that are observed before and after the occultation event. These two burst are individually asymmetric under time reversal, although they are mirror images of each other. In the first burst, the observed flux increases towards a divergency and then drops to zero. The infinity, or “caustic”, and the vertical drop to zero are consequences of the ideal model adopted in the calculations, with a point source at the background. A more realistic model should consider an extended source with a given intensity distribution over it.

Recently, Anchordoqui et al. [6] searched in existent gamma-ray bursts databases for signatures of wormhole microlensing. Although they detected some interesting candidates, no conclusive results could be obtained. Peculiarly asymmetric gamma-ray bursts [7], although highly uncommon, might be probably explained by more conventional hypothesis, like precessing fireballs (see, for instance, Ref. [8]). Even in the case of galactic microlensing, highly asymmetric curves can be the effect of microlensing by binary stellar systems [9]. Hence, although binary lenses produce asymmetric lightcurves with different shapes than those that would be produced by wormholes, discriminators other than the lightcurves are needed in order to identify wormhole microlensing events.

In this paper, we expand the analysis of Cramer et al. [3] and Torres et al. [4] to the extended source case. This allow us to present more realistic lightcurves for wormhole microlensing events. Then, using this formalism, we compute the effects of a finite source extent on the spectral features of microlensing. We show that limb darkening of the intensity distribution on a stellar source induces specific chromaticity effects that are very different from what is expected in the positive mass lens case. Thus, multi-color optical observations can be used to search for galactic natural wormholes. In addition, we study the extragalactic wormhole microlensing of background AGNs taking into account the variations of the source size with the observing wavelengths. This extends the previous work by Torres et al. [4], who first considered these kind

of events at gamma-rays adopting a point-like source. We show that also in this case the spectral evolution during the wormhole microlensing event presents peculiar signatures that allow its identification.

2 Microlensing by wormholes in the extended source case

The total amplification $A = I_{\text{obs}}/I_0$ —where $I_{\text{obs}}(I_0)$ is the observed (intrinsic) luminosity—of a background point source due to gravitational lensing by a single point mass is given by [3]

$$A_0 = \frac{B_0^2 \pm 2}{B_0 \sqrt{B_0^2 \pm 4}}, \quad (1)$$

where the plus (minus) sign corresponds to the positive (negative) mass case, and

$$B_0 = \frac{b_0}{R_E} \quad (2)$$

is the shortest lens-source separation (on the lens plane) in units of the Einstein ring radius, R_E , defined as

$$R_E = \sqrt{\frac{4G|M|}{c^2} \frac{D_{\text{ol}} D_{\text{ls}}}{D_{\text{os}}}}. \quad (3)$$

In this last expression, D_{os} is the observer-source distance, D_{ol} is the observer-lens distance, D_{ls} is the lens-source distance, and M is the mass of the gravitational lens.¹

When the source is extended, we must take into account the contributions coming from the different parts of it. The amplification observed at a frequency ν , then, results:

$$A_\nu = \frac{\int_0^{2\pi} \int_0^{r_*} \mathcal{I}_\nu(r, \varphi) A_0(r, \varphi) r dr d\varphi}{\int_0^{2\pi} \int_0^{r_*} \mathcal{I}_\nu(r, \varphi) r dr d\varphi}, \quad (4)$$

where (r, φ) are polar coordinates in a reference frame centered in the source (e.g. a star), r_* is the radius of the source and $\mathcal{I}_\nu(r, \varphi)$ is its surface intensity distribution. For a radially symmetric distribution we have:

$$A_\nu = \frac{\int_0^{2\pi} \int_0^{r_*} \mathcal{I}_\nu(r) A_0(r, \varphi) r dr d\varphi}{2\pi \int_0^{r_*} \mathcal{I}_\nu(r) r dr}. \quad (5)$$

If the lens is moving with constant velocity v , the lens-source separation evolves in time as

$$b(t) = \sqrt{(b_0 + r \sin \varphi)^2 + (-vt + r \cos \varphi)^2}. \quad (6)$$

In the published version of this paper, this is illustrated in the first figure. In units of the Einstein radius, we have:

$$B(T) = \frac{b(t)}{R_E} = \sqrt{(B_0 + R \sin \varphi)^2 + (-T + R \cos \varphi)^2}, \quad (7)$$

where $T = vt/R_E$. Replacing now B_0 by $B(T)$ in Eq. (1), we obtain the time dependent amplification.

¹It should be kept in mind that any form of negative masses, not only wormholes, would produce the same observational effects.

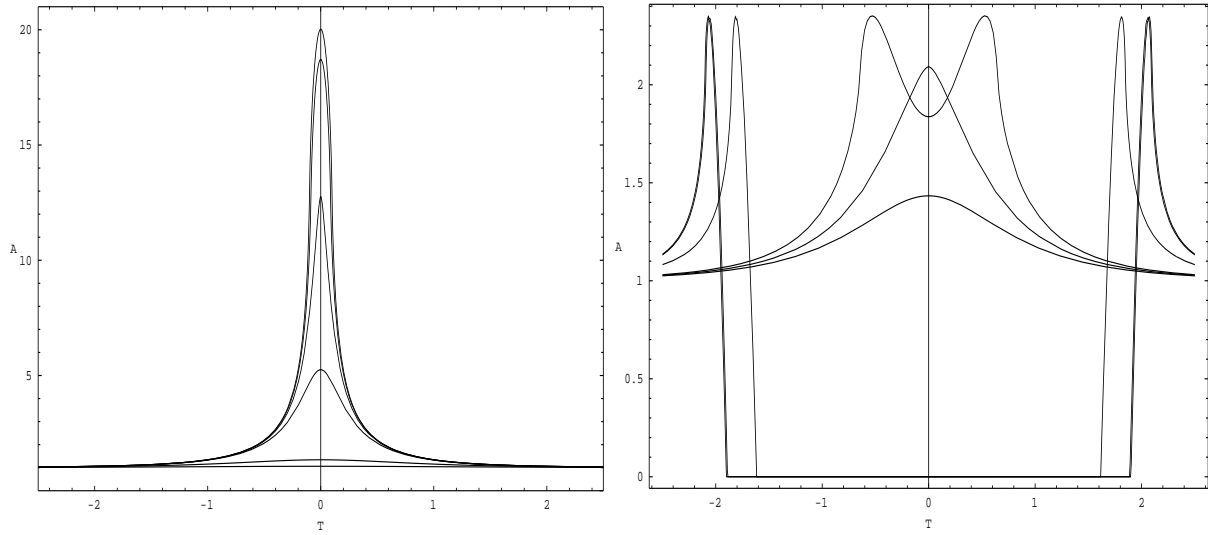


Figure 1: Lightcurves for a microlensing event of a background extended source produced by a positive point mass (left panel) and a negative point mass (right panel). The vertical axis gives the total amplification of the background intensity. The different curves are for different impact parameters [$k=0, 0.5, 1, 2, 10,$ and $20,$ from top to bottom, in the case of positive lensing; and $k=0$ and 2 (in the same curve), $10, 20, 21,$ and $22,$ from left to right, in the case of negative lensing]. See text for additional details.

In order to compute the expected lightcurves for the case of negative mass lenses, we take the negative sign in Eq. (1) and replace it in Eq. (5). In Figure 2 we show different lightcurves for different impact parameters, calculated assuming a circular source of uniform brightness and radius $R_* = r_*/R_E = 0.1$. These curves should be compared with the ideal curves presented by Torres et al. [4] in their Figure 1. The main difference is that in the extended source case the divergencies are eliminated, and there is not a discontinuous transition to or from the umbra region. The basic features of the microlensing event, however, remain. For $B_0 < 2$, we have two successive intensity enhancements, separated by a period of absence of radiation. The individual bursts are quite asymmetric. In the case $B_0 > 2$, there is only one event, symmetric under time reversal and similar to what is observed in the standard case.

Real background sources in microlensing events can present non-uniform brightness distributions on their surfaces and a dependency of their emission with the observing frequency. These complications can result in chromaticity effects, i.e. in spectral changes induced by differential lensing during the event. In the next sections we shall compute such changes in order to establish whether they can provide a specific signature of wormhole microlensing.

3 Chromaticity effects in microlensing of stars

Stars are brighter in their center. The obscuration of the intensity profile of a star towards its border is known as “limb darkening”. They also radiate as a blackbody with an effective temperature T_{eff} , and consequently their emission is frequency dependent. To compute the chromaticity effects due to these characteristics, we represent the intensity profile of typical star by [11]:

$$\mathcal{I}_\nu(r) = 1 - C_\nu \left(1 - \sqrt{1 - \left(\frac{r}{r_*}\right)^2} \right), \quad (8)$$

where the limb-darkening coefficients in the I and U bands can be taken as $C_{\nu_1} = 0.503$ and $C_{\nu_2} = 1.050$, respectively, for a K-giant star with $T_{\text{eff}} = 4750\text{K}$.

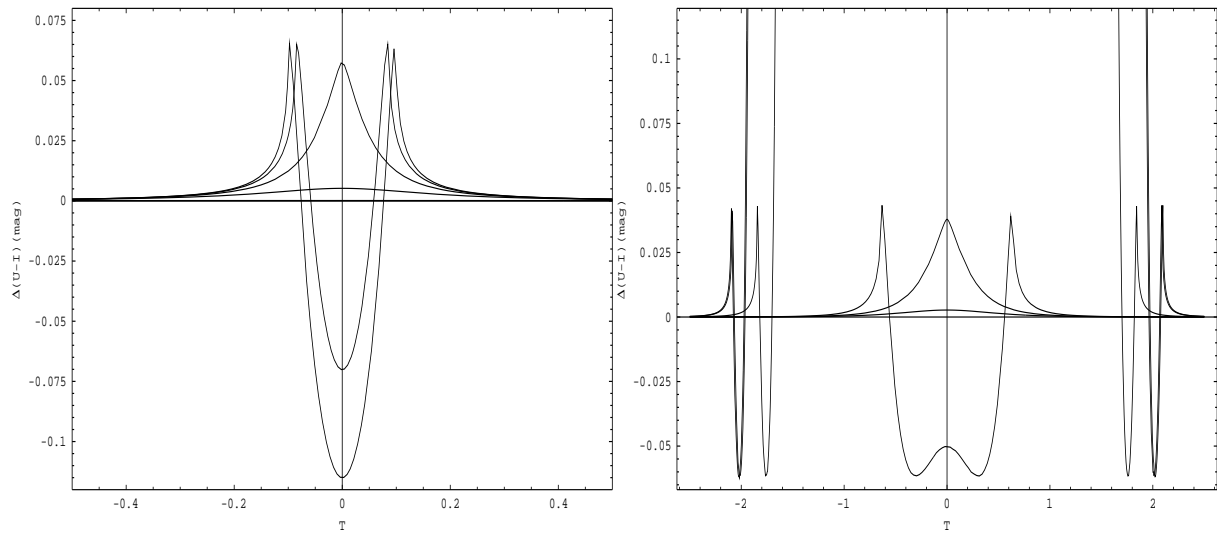


Figure 2: Color curves for a microlensing event of a background extended source of variable surface brightness produced by a positive point mass (left panel) and a negative point mass (right panel). The different curves are for the same impact parameters as in Figure 2. In the case of negative mass lensing, from left to the right, $k=0$ and 2 (in the same curve), 10, 20, 21, and 22. In the case of the positive mass lensing, from left to right, $k=0, 0.5, 1, 2, 10$ and 20 (the latter two in the same curve). See text for additional details.

Defining the dimensionless radius as $R = r/R_E$, we obtain

$$A_\nu = \frac{\int_0^{2\pi} \int_0^{R_*} \mathcal{I}_\nu(R) A_0(R, \varphi) R dR d\varphi}{2\pi \int_0^{R_*} \mathcal{I}_\nu(R) R dR} \quad (9)$$

and

$$\mathcal{I}_\nu(R) = 1 - C_\nu \left(1 - \sqrt{1 - \left(\frac{R}{R_*} \right)^2} \right), \quad (10)$$

where $R_* = r_*/R_E$ is the dimensionless radius of the star. The colour change caused by limb darkening can then be computed by [11]

$$\Delta(m_{\nu_1} - m_{\nu_2}) = -2.5 \log \left(\frac{A_{\nu_1}}{A_{\nu_2}} \right). \quad (11)$$

In Figure 3 we show several color curves for both positive (left panel) and negative (right panel) mass lenses. The different curves correspond to different impact parameters $k = B_0/R_*$ specified in the caption. The star radius was considered, as before, equal to $R_* = 0.1$. In the case of an ordinary lens, we see that as it gets closer to the star, the color of the observed source becomes redder due to the differential amplification of the coldest regions. When the lens transits towards the star interior, the hot center starts to dominate the amplification, producing a dramatic change in the slope of the color curve. This is basically the result recently found by Han et al. [11].

If we now look at the color curves for the negative mass lens case, we notice a clear contrast in the behaviour. The spectral changes start long before than in the standard situation. Initially, the source also becomes redder and then experiences a switch when shorter wavelengths begin to dominate. Contrary to what happens with positive masses, the spectral trend changes again, with the source appearing colder and colder until it vanishes in the umbra during the transit. When the source is seen again, the inverse behaviour is observed.

4 Chromaticity effects in extragalactic microlensing

Let us now turn to the extragalactic microlensing case, which was previously studied by Torres et al. [4] using point sources. We shall study the lightcurves produced by a stellar-mass extragalactic wormhole when it crosses the line of sight to a background compact source, namely and Active Galactic Nuclei (AGN). As discussed by Torres et al. [4], a critical requirement to observe a significant light magnification during the microlensing event is that the size of the source, when projected onto the lens plane, is not larger than the Einstein ring of the lensing mass. This is necessary because otherwise light from outside the ring could become dominant and smooth out the gravitationally induced variability. In the case of an AGN, since the size of the emitting regions varies with the wavelength, the gravitational amplification will be more effective at those wavelengths at which the source is more compact. The wavelengths where the amplifications are maximized are located at gamma-ray energies [4].

The compactness of the gamma-ray central region of an AGN is determined by the opacity to the propagation of gamma-ray photons in the X-ray field produced by the object. Since the opacity is a function of the photon energy, the size of the observable gamma-ray photosphere will also depend on the observing energy. Differential amplification during the microlensing event, then, should lead to chromaticity effects. In order to compute these effects, we shall adopt a radius of the photosphere given by the maximum height at which photons of energy E are absorbed by pair creation in the X-ray radiation field of the inner accretion disk. According to Becker & Kafatos [10], this size is

$$r_\gamma \propto E^{\alpha/(2\alpha+3)}, \quad (12)$$

where α is the X-ray spectral index of the accretion disk radiation field. In our calculations, we shall adopt an average value $\alpha = 1.1$ [12]. The larger photospheres, then, are those observed at the higher energies. To compute the microlensing effects on the AGN, we define a reference source with radius r_{ref} and gamma-ray energy E_{ref} , such that

$$R_\gamma(E) = R_{\text{ref}} \left(\frac{E}{E_{\text{ref}}} \right)^{\alpha/(2\alpha+3)}, \quad (13)$$

where we have written r_γ and r_{ref} in units of the Einstein radius R_E .

The intensity of the source (without lensing) is uniform and its spectrum follows approximately a power law:

$$I_0(E) \propto E^{-\xi} \quad (14)$$

with ξ typically in the range $\xi \in (1.7, 2.7)$. We can write this latter Eq. in the form:

$$I_0(E) = I_{\text{ref}} \left(\frac{E}{E_{\text{ref}}} \right)^{-\xi}, \quad (15)$$

where I_{ref} is the intensity of the reference source. The surface intensity distribution is assumed to be constant at a given energy

$$\mathcal{I}_0(E) = \frac{I_0(E)}{\pi (R_\gamma(E))^2}. \quad (16)$$

Then, the total amplification of the source due to microlensing can be computed as

$$A = \frac{I}{I_0} = \frac{\int_0^{2\pi} \int_0^{R_\gamma(E)} \mathcal{I}_0(E) A_0(R, \varphi) R dR d\varphi}{\int_0^{2\pi} \int_0^{R_\gamma(E)} \mathcal{I}_0(E) R dR d\varphi}. \quad (17)$$

Since $\mathcal{I}_0(E)$ does not depend on (R, φ) , we have

$$A = \frac{\int_0^{2\pi} \int_0^{R_\gamma(E)} A_0(R, \varphi) R dR d\varphi}{\pi (R_\gamma(E))^2}. \quad (18)$$

From Eq. (15) and Eq. (17) we obtain:

$$I = AI_0 = AI_{\text{ref}} \left(\frac{E}{E_{\text{ref}}} \right)^{-\xi}. \quad (19)$$

Let us now introduce the dimensionless minimum impact parameter k as:

$$k = \frac{B_0}{R_\gamma(E)}. \quad (20)$$

Adopting $\xi = 2$, $R_{\text{ref}} = 0.2$, and $E_{\text{ref}} = 100$ MeV, we can use Eq. (18) and Eq. (19) to compute the expected lightcurves and the spectral evolution during the microlensing event. The results are shown, for a variety of impact parameters, in Figures 4-7, where we define J as the ratio between I and I_{ref} .

The main point to be emphasized in the spectral evolution of the lensed source is that, when the source is a wormhole, the spectrum emerges from the umbra at its lowest level (the bottom curve in the spectral plots) and then it jumps to its maximum, from where it decreases slowly keeping its slope in the log-log diagram. This occurs because after the transit the intensity have to recover from the umbra null values. The effects of the differential obscuration also appear as a clear break in the spectrum at early times since the transit. This break, with a hardening at low energies, results because the smaller and less energetic gamma-spheres emerge from the umbra after than the more energetic (and bigger) ones, and then are initially less amplified. The break in the spectrum is best appreciated in Figure 6, where the impact parameter is $k = 1$.

In the case of positive lenses (upper set of panels in the figures) the evolution is smoother, decreasing the emission at all wavelengths after the transit. The chromaticity effects in this case are limited to a small slope change at medium energies.

5 Concluding remarks

In this paper we have developed the formalism for gravitational microlensing of extended sources when the lens is a wormhole-like object. We have studied the chromaticity effects introduced by the finite source size and the non-uniform intensity distribution on it, finding a set of very peculiar features that allow a clear identification of any lens having a negative energy density. These chromaticity effects, when combined with the observed lightcurves, provide a unique tool to study the possible existence of natural wormholes in the universe.

Acknowledgments

This work has been supported by Universidad de Buenos Aires (UBACYT 01TW77, EE), CONICET (DFT, and PIP 0430/98, GER), ANPCT (PICT 98 No. 03-04881, GER), and Fundación Antorchas (GER and DFT).

References

- [1] M. S. Morris & K. S. Thorne, *Am. J. Phys.* **56**, 395 (1988).
- [2] D. Hochberg & M. Visser, *Phys. Rev. Lett.* **81**, 746 (1998); *Phys. Rev D***58**, 044021 (1998); *Phys. Rev. D***56**, 4745 (1997); E. E. Flanagan & R. M. Wald, *Phys. Rev. D***54**, 6233 (1996); L. A. Anchordoqui, S. E. Perez Bergliaffa & D. F. Torres, *Phys. Rev. D***55**, 5226 (1997); C. Barceló & M. Visser, *Phys. Lett. B***466**, 127 (1999).
- [3] J. G. Cramer, R. L. Forward, M. S. Morris, M. Visser, G. Benford, G. A. Landis, *Phys. Rev. D***51**, 3117 (1995).
- [4] D. F. Torres, G. E. Romero & L. A. Anchordoqui, *Phys. Rev. D***58**, 123001 (1998); D. F. Torres, G. E. Romero & L. A. Anchordoqui, (*Honorable Mention, Gravity Foundation Research Awards 1998*), *Mod. Phys. Lett. A***13**, 1575 (1998).
- [5] M. Safonova, G. E. Romero & D. F. Torres, *Mod. Phys. Lett. A***16**, 153 (2001) [astro-ph/0104075].
- [6] L. A. Anchordoqui, G. E. Romero, D. F. Torres & I. Andruchow, *Mod. Phys. Lett. A***14**, 791 (1999).
- [7] G.E. Romero, D.F. Torres, L.A. Anchordoqui, I. Adruchow, B. Link, *Monthly Notices Royal Astron. Soc.* **308**, 799 (1999).
- [8] S. F. Portegies Zwart, C-H. Lee, H.K. Lee, *Astrophys. J.* **520**, 666 (1999).
- [9] A. Udalski, M. Szymański, S. Mao, et al., *Astrophys. J.* **436**, L103 (1994).
- [10] P.A. Becker, M. Kafatos, *Astrophys. J.* **453**, 83 (1995).
- [11] C. Han, S-H. Park, J-H. Jeong, *Monthly Notices Royal Astron. Soc.* **316**, 97 (2000).
- [12] J.H. Krolik, *Active Galactic Nuclei*, (Princeton University Press, Princeton, 1999).

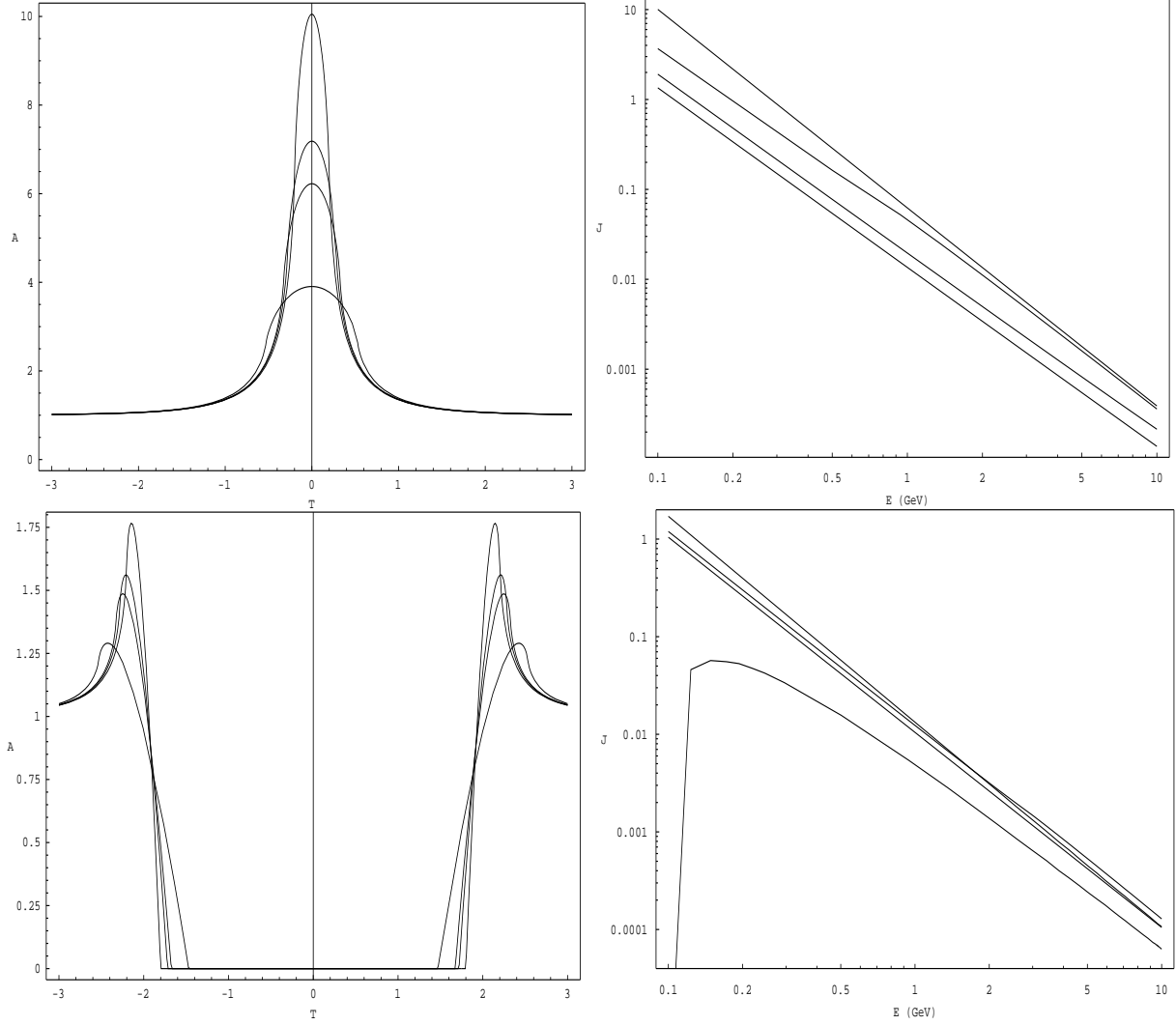


Figure 3: Lightcurves (on the left) for a microlensing event of a background gamma-ray emitting AGN produced by a positive point mass (upper panel) and a negative point mass (lower panel). Impact parameter $k = 0$. The different curves correspond to the amplification of different regions in the object. The energies considered were 10GeV, 1GeV, 500MeV, and 100MeV, and correspond, both for positive and negative lensing, to the curves depicted on the left diagrams from bottom to top. The corresponding spectral changes for the entire source are shown in the panels on the right side. For the positive case the spectra evolve from the top to downwards as time increases from $T = 0$ to $T = 1$. In the negative case, instead, the evolution of the curves with time is given by, from top downwards, $T = 2.1$, $T = 2.4$, $T = 3.0$, and finally the curve for $T = 1.8$. See text for further explanation.

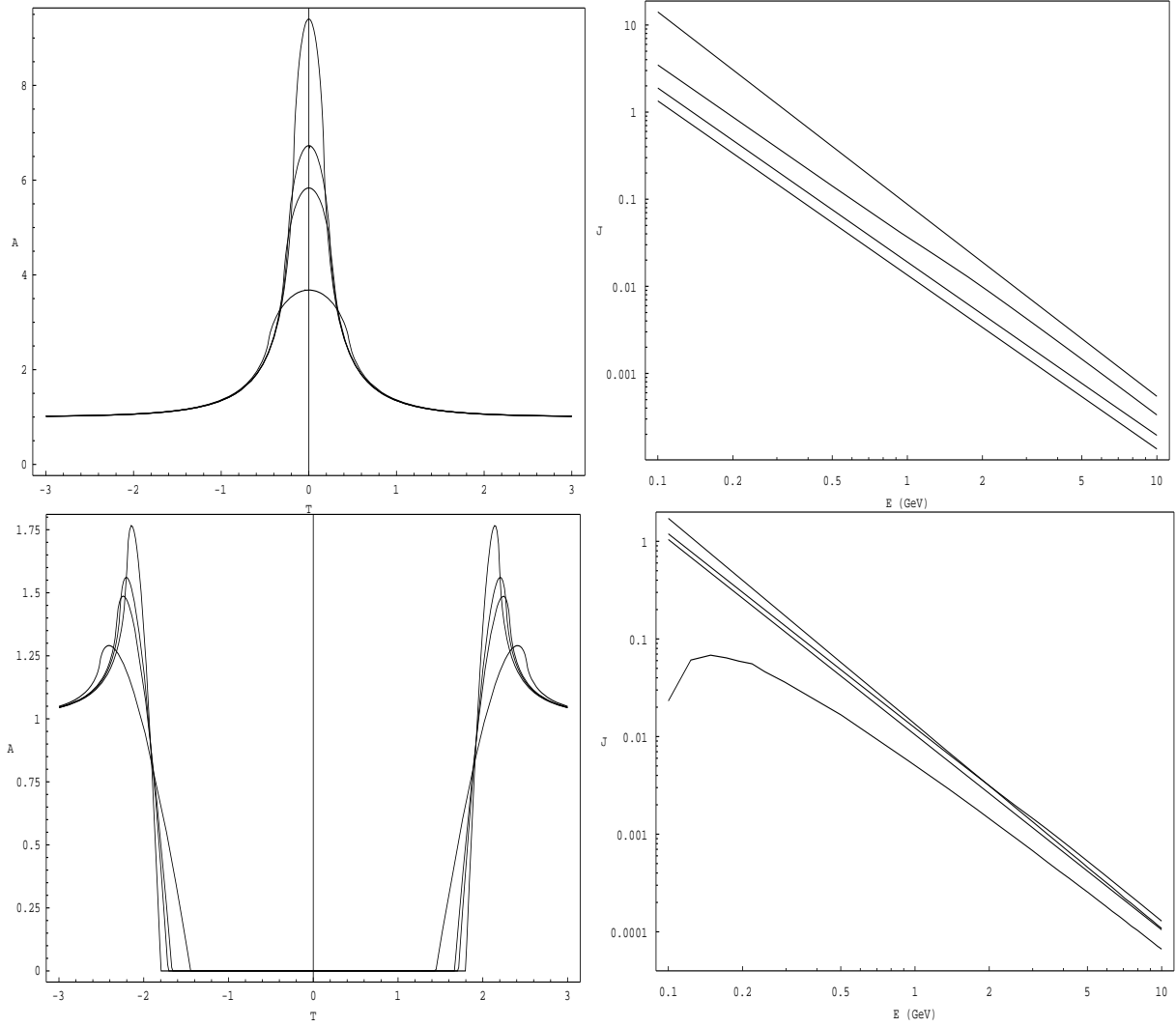


Figure 4: Idem Fig. 4, but for $k = 0.5$

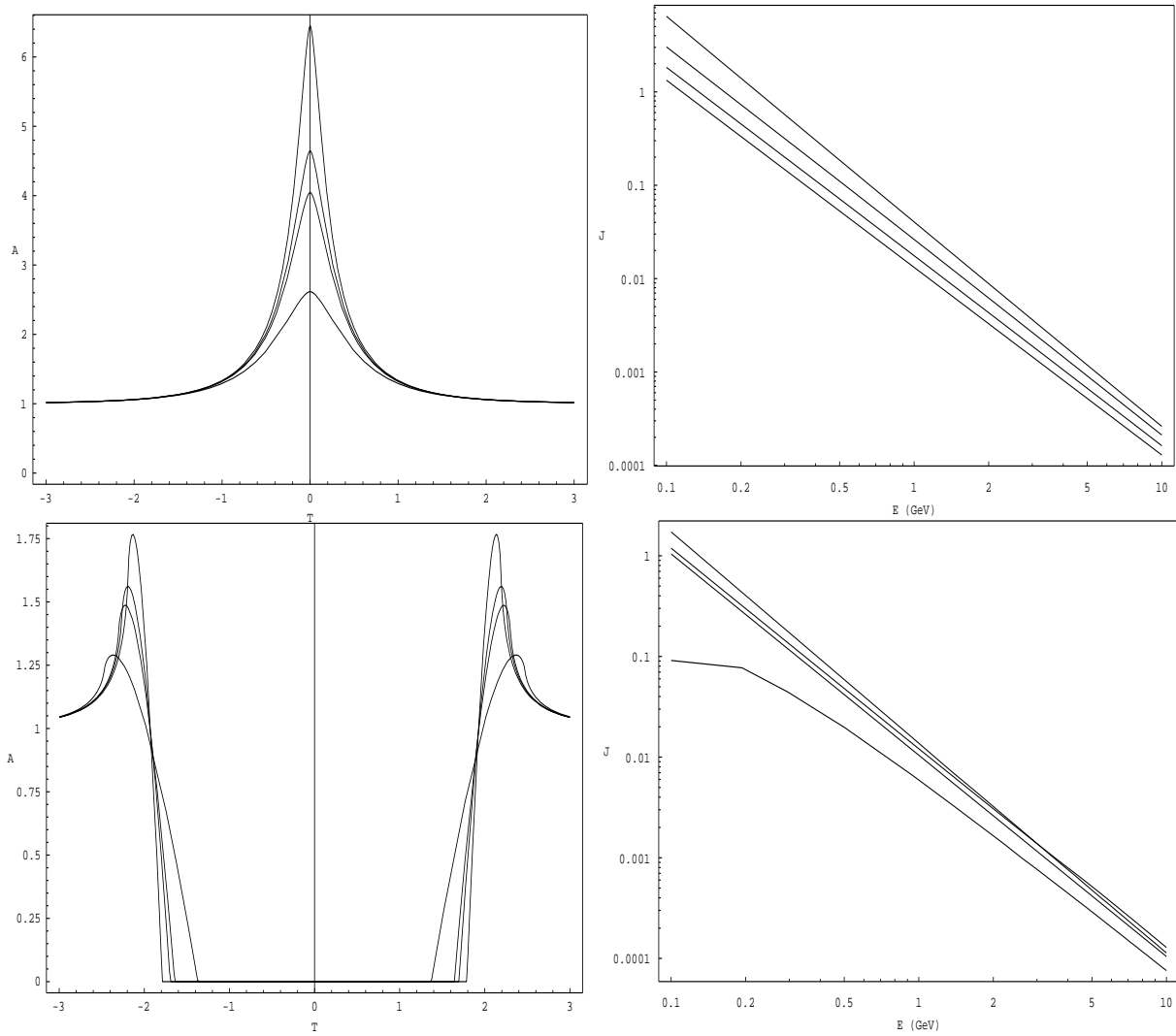


Figure 5: Idem Fig. 4, but for $k = 1$

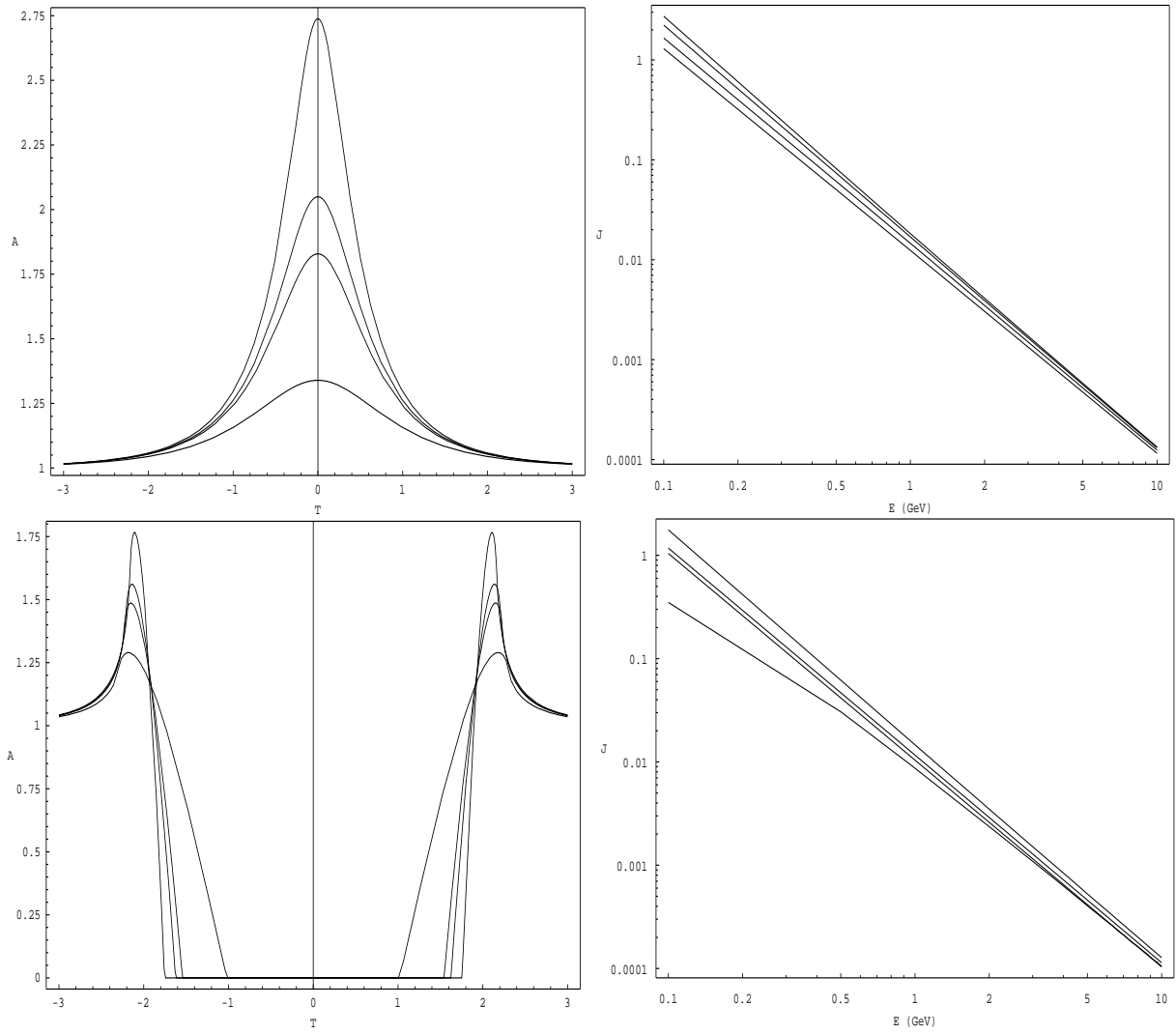


Figure 6: Idem Fig. 4, but for $k = 2$